Journal of Magnetic Resonance **144,** 108–114 (2000)
doi:10.1006/jmre.2000.2026, available online at http://www.idealibrary.com on IDEAL®

Relaxation Effects on Transverse Magnetization Using RF Pulses Long Compared to T_2

Antonella Raddi and Uwe Klose

Division of Experimental NMR of CNS, Department of Neuroradiology, University of Tübingen, Hoppe-Seyler Strasse 3, D-72076 Tübingen, Germany

Received September 10, 1999; revised January 18, 2000

The transverse relaxation effects which occur during the application of optimized slice-selective Shinnar–Le Roux pulses are studied. The behavior of both longitudinal and transverse magnetization is examined, focusing the attention on changes which affect the absorption and dispersion components. Besides the reduction in amplitude, the absorption component was found to be unaffected by transverse relaxation times, whereas the dispersion component was strongly distorted. A comparison between the distortion components from pulses having same length but different bandwidths is given. © 2000 Academic Press

Key Words: **SLR pulses; relaxation; absorption; dispersion; bandwidth.**

INTRODUCTION

Some NMR applications require RF pulses with duration of the same magnitude of relaxation times, precluding the possibility of ignoring relaxation during the pulse itself. It is therefore necessary to study the effects of relaxation times on the magnetization profiles. Only a few papers have been written about this topic.

Norris *et al.* (*1*) analyzed the effects of short T_2 values on selective inversion hyperbolic-secant pulses, reporting a noticeable effect of reduction in the magnetization outside the slice. In 1993, Hajduk *et al.* (*2*) examined the influence of relaxation on the frequency-domain profiles of a variety of both excitation and inversion pulses, using both infinite and short T_1.

The results reported in (*2*) are very similar to those described in (*1*): decay of the on-resonance magnetization and a significant degradation of the frequency profiles, especially when short T_1 relaxation times were assumed. In any case, the effects of longitudinal relaxation time were not as significant with short T_2.

In their papers, both Norris *et al.* and Hajduk *et al.* focused their attention on the profiles of the longitudinal and transverse magnetization. On the contrary, it can be very important to study the behavior of all the magnetization components to investigate their mutual interactions and to study whether and how changes in one of the three components could affect the behavior of the others.

Optimized Shinnar–Le Roux (SLR) pulses (*3, 4*), calculated neglecting relaxation times, have very good frequency profiles. They have been used in conventional FSE sequences, replacing optimized sinc-pulses, inducing not only signal improvement, but even contrast enhancement (*5*).

The effects of short relaxation times on optimized SLR pulses have not yet been analyzed. The aim of this paper is to study the T_2 relaxation effects on optimized 90° SLR pulses having same length but different bandwidths, without T_1 relaxation effects. The behavior of all three components is analyzed, with special attention to absorption and dispersion components of the transverse magnetization.

Neglecting T_1 is a very common assumption and, because of the large ratio of T_1 to T_2 in many brain tissues, it is not too strict a constraint. This assumption is not true for fluids like CFS, but in this case relaxation times are in the range of seconds and therefore much longer than the RF pulse duration.

METHODS

We generated three optimized 90° Shinnar–Le Roux pulses (*3, 4*), with a duration of $L = 1.024$ ms, bandwidths of 2.5, 5.0, and 7.5 kHz, and 0.1% pass and stopband ripples. A modified version of Matpulse-1.0 (see Matson (*6*)) has been used to obtain optimized SLR pulses. They have one, three, and five lobes, respectively. In every case, we used 512 time steps.

To calculate the magnetization profile, a sequence of RF pulse and gradient pulses—a field gradient G_0 for slice selection and a refocusing gradient G_{ref}—has been simulated by the Bloch equations with relaxation terms. They have been numerically solved by the fourth-order Runge–Kutta method (*7, 8*). To excite a 10-mm slice, the following values for the amplitude of the slice-selective gradient have been used: 5.0, 10.0, and 15.0 mT/m, respectively, for pulses with bandwidth of 2.5, 5.0, and 7.5 kHz.

The amplitude and length of the selective gradient have been left fixed, as well as the length of the refocusing gradient G_{ref}, whereas the amplitude of G_{ref} has been modified in order to obtain the maximum signal without reinforcing the relaxation time effects. The magnetization profiles have been calculated directly after the end of the refocusing gradient.

We wanted to study the behavior of the magnetization pro-

1090-7807/00 $35.00

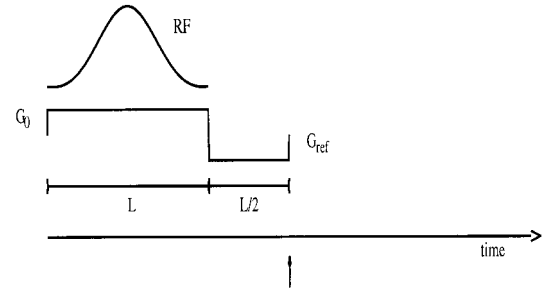

FIG. 1. Assumed sequence for the performed simulation. The z gradient is shown with a slice selection gradient amplitude G_0 and a refocusing gradient amplitude G_{ref} which changes in different simulations. The duration L of the slice selection gradient and the duration $L/2$ of the refocusing gradient are left fixed. The upward arrow points to the time when the magnetization has been calculated.

file from pulses with lengths comparable to the transverse relaxation times. For that reason, we used four different values of T_2: infinity, $2L$, L, and $L/2$, where L is the length of the pulse. When relaxation times different from infinity were used, the longitudinal magnetization on-resonance was not zero. In order to have no longitudinal component on-resonance, the longitudinal magnetization has been adjusted by using flip angles larger than 90°.

The magnetization profiles have been determined both in case of retuning of the pulse power (zero on-resonance M_z) and in case of nonzero on-resonance longitudinal magnetization, if applying nominal 90° pulses. The absorption and dispersion components calculated with small values of T_2 have been compared to the same components calculated with $T_2 = \infty$.

One major effect of short T_2 relaxation time is the exponential decay of the transverse magnetization after the maximum of the RF pulse. All of the other effects can be better focused if a normalization of the two components is performed. That has been done by dividing both M_x and M_y by the maximum of the transverse magnetization M_{xy}.

The intensity of the NMR signal is directly dependent on the value of both absorption and dispersion components of the transverse magnetization. Actually, it is given by the absolute value of the sum of the overall contribution of M_x and M_y in every single point of the slice excited. In order to calculate the signal intensity, the sample must be assumed to be homogeneous. That means it is characterized by the same relaxation times and proton density in every point. The integrals of the absorption and dispersion components over space have been calculated by the trapezoidal rule (*7, 8*).

After being excited by an RF pulse, the transverse magnetization begins to dephase because of the slice-selective gradient. A refocusing gradient is used to let the magnetization rephase. The length and the amplitude are usually set to half the length of the pulse and to the negative amplitude of the selective gradient, respectively. It has been proved that a rephasing interval slightly different from $L/2$ improves the phase behavior when relaxation is neglected (*9*). Here we keep the length fixed and change the amplitude of the refocusing gradient to the value which yields the maximum signal intensity.

In order to compare the results obtained for different pulses and T_2 values, the ratio between the optimal refocusing gradient (calculated to obtain the maximum signal) and the gradient amplitudes has been evaluated. The percentage of signal gained or lost compared to the signal obtained by using the negative value of the selective gradient as a refocusing gradient has been also calculated.

RESULTS

The profiles in space domain have been calculated by using the simulated sequence of RF and gradient pulses shown in Fig. 1. Three different optimized 90° SLR pulses, plotted in Fig. 2, have been applied together with a selective gradient G_0, followed by a refocusing gradient G_{ref} having half the length of the selective gradient and different amplitude depending on the pulse, the nominal flip angle, and the T_2 time.

The absorption, dispersion, and longitudinal components of the profile from the 90° pulse with bandwidth of 2.5 kHz are plotted in Fig. 3. The components calculated using relaxation times smaller than infinity are compared with those calculated with an infinite T_2. In the four columns of the figure, the three

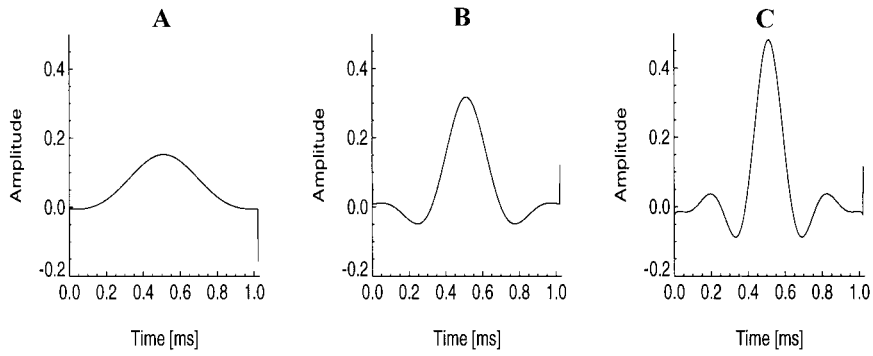

FIG. 2. Optimized 90° SLR pulses with the same length $L = 1.024$ ms, but different bandwidths: (A) 2.5 kHz; (B) 5 kHz; (C) 7.5 kHz.

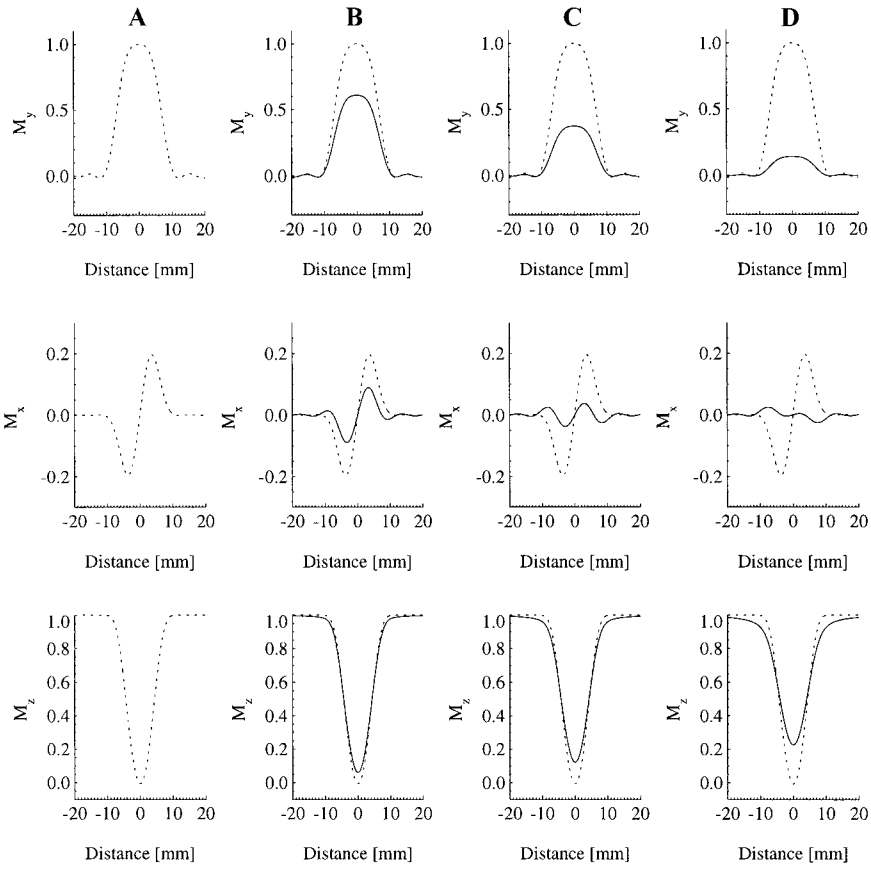

FIG. 3. Relaxation effects on magnetization profiles relative to the pulse with a 2.5-kHz bandwidth assuming different T_2 values. The absorption and dispersion components, as well as the longitudinal magnetization, calculated using (A) $T_2 = \infty$ (dashed) and those calculated using (B) $T_2 = 2L$; (C) $T_2 = L$; (D) $T_2 = L/2$ (solid) are compared here. L is the length of the pulse.

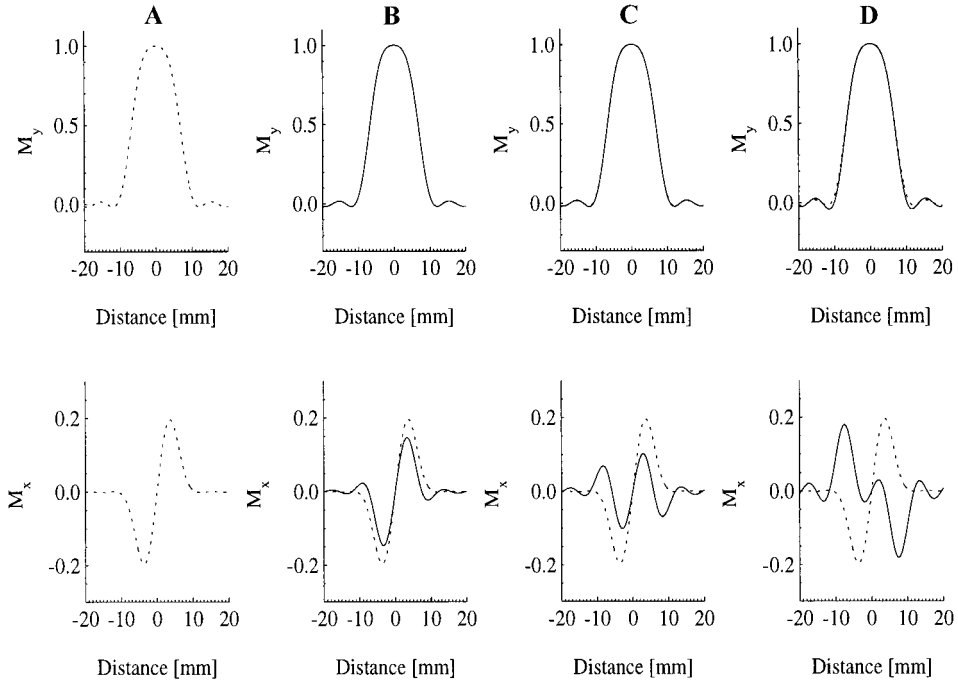

FIG. 4. Absorption and dispersion components, normalized to the maximum of the transverse magnetization M_{sy}, calculated assuming T_2 values less than ∞ are compared to the M_y and M_x components calculated by using $T_2 = \infty$. (A) $T_2 = \infty$; (B) $T_2 = 2L$; (C) $T_2 = L$; (D) $T_2 = L/2$, where L is the length of the pulse.

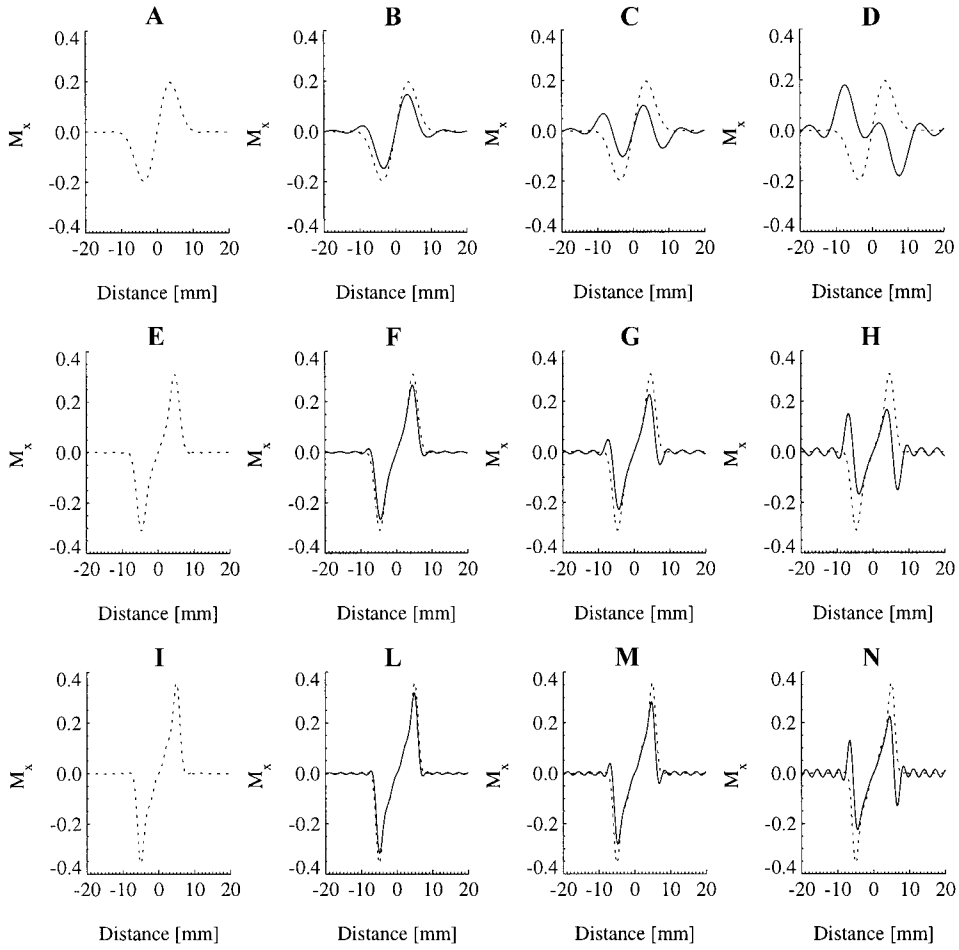

FIG. 5. M_x components normalized to the maximum of M_{xy}. The dispersion component calculated with $T_2 = \infty$ (dashed line) is here compared with the same components calculated with $T_2 = 2L$, $T_2 = L$, $T_2 = L/2$ (solid line). 2.5 kHz (A–D), 5.0 kHz (E–H), 7.5 kHz (I–N). L is the length of the pulse.

components of the magnetization profile calculated for different relaxation times are shown. As expected, every component has a reduced amplitude when values of T_2 different from infinity are used. The longitudinal component does not change only in amplitude, but even in shape. The transition band becomes wider when the relaxation time is smaller, exciting parts of the sample which are out of the slice to be selected.

The absorption and dispersion components from the same pulse are shown in Fig. 4. Here they are both normalized to the maximum of the transverse magnetization M_{xy}. The normalized M_y component does not change its shape when values of T_2 greater than or equal to the length of the pulse are used. If $T_2 = L/2$, a slight distortion can be detected (Fig. 4D). The most evident effect on M_x is that the dispersion component changes its shape: the linear behavior is reduced in the central part of the profile and a larger number of oscillations appears.

The behavior of optimized 90° SLR pulses with the same length (1.024 ms), but with different bandwidths (5.0 and 7.5 kHz) has been studied. In both cases, as well as for the pulse with a 2.5-kHz bandwidth, the absorption component amplitude is reduced. In Fig. 5, the dispersion components of the three kinds of pulses have been plotted. If the bandwidth is larger, that is if the magnetization profile has a more rectangular shape, the normalized x components undergo a weaker amplitude reduction and show side oscillations with higher frequency, but smaller amplitude.

Examinations have been performed to analyze whether a refocusing amplitude different from $-G_0$ could reduce the dephasing influence of the M_x component and therefore induce a better signal. This has been done in different conditions for every pulse. In order to have a zero longitudinal magnetization on-resonance, it is possible to retune the pulse power by adjusting the flip angle. In Table 1, the adjusted values for every pulse are shown. The larger the bandwidth is, the less the flip angles have to be modified.

In Tables 2 and 3, the results relative to the pulse with a 2.5-kHz bandwidth are shown. They have been obtained keeping the flip angle fixed to the maximum value, which means that the longitudinal magnetization on-resonance is not zero when T_2 times smaller than infinity are used (Table 2), and adjusting the magnetization by changing the flip angle to have zero M_z component on-resonance (Table 3).

To obtain the maximum signal in case of 90° flip angle, the relative refocusing amplitude had to be increased to +5.8% if

TABLE 1
Adjusted Flip Angles for Different T_2 Values

	Flip angle		
T_2	2.5 kHz	5.0 kHz	7.5 kHz
∞	90.0°	90.0°	90.0°
$2L$	94.1°	91.2°	90.5°
L	98.3°	92.5°	91.2°
$L/2$	107.0°	95.1°	92.6°

$T_2 = \infty$ and decreased to -8.8% if $T_2 = L/2$ (Table 2). After adjusting the longitudinal magnetization, the maximum signal has been reached increasing the refocusing amplitude to only slightly different values (Table 3). The maximum signal gain can be obtained with an accuracy of $\pm 0.1\%$ using a range of relative refocusing amplitudes. In both tables, such a range is given in the column Relative refocusing amplitude range.

In Fig. 6, the signal percentage calculated in case of a pulse with 2.5-kHz bandwidth and $T_2 = \infty$ and $T_2 = L/2$ is plotted. The signal gain in both cases has been shown. It can be seen that the optimal signal intensity can almost be reached within a range of 2.5–3% of G_{ref}. However, the ranges of G_{ref} values for the examined T_2 values do not overlap.

The same calculation has been performed for the pulses with 5.0- and 7.5-kHz bandwidth. The relative refocusing amplitude and the signal gain relative to the three pulses are given in Table 4 (nonzero longitudinal magnetization on-resonance, after 90° pulses have been applied) and in Table 5 (adjusted longitudinal magnetization). In both cases, there is a stronger signal gain for pulses with better magnetization profiles when T_2 times greater than or equal to the pulse length are used. When $T_2 = L/2$, the signal gain is much larger for the pulse whose bandwidth is 2.5 kHz.

DISCUSSION

In the studies previously performed, the effects of relaxation on the frequency-domain profiles from a variety of both excitation and inversion pulses have been analyzed (*1*, *2*). Attention has been especially focused on the T_2 relaxation effects, assuming an infinite T_1 time. In Hajduk *et al.* (*2*) simulations have been performed even with $T_1 = T_2$.

Different effects have been reported, both quantitative and qualitative: the simulated magnetization profiles—in the case of both excitation and inversion pulses—were reduced and degraded. The shorter the T_1 time was, the more degraded the frequency profiles were. A reduction in the magnetization outside the slice was also reported.

In order to avoid T_1 effects interferences, we performed all our simulation by assuming an infinite longitudinal relaxation time. The calculation of magnetization profiles—performed using the simulated sequence of RF and gradient pulses shown in Fig. 1—has pointed out the reduction in the longitudinal magnetization outside the slice already reported by Norris *et al.* (*1*) and Hajduk *et al.* (*2*). The same effect has been detected using the RF pulses with the same duration and different bandwidths plotted in Fig. 2.

Studying at the same time the behavior of the absorption and dispersion components from the pulse having a 2.5-kHz bandwidth, besides the reduction in amplitude, a noticeable distortion in the dispersion component has been detected (see Fig. 3). After the M_y and M_x components have been normalized (Fig. 4), it becomes clear that the distortion in the dispersion component profiles involves points which are out of the slice to be selected, whereas the absorption component is unaffected.

In our simulation, we found that the longitudinal and the dispersion components from pulses with larger bandwidth and more rectangular magnetization profiles undergo a smaller reduction and distortion, respectively. A correlation between the reduction in the longitudinal magnetization outside the slice with the distortion in the M_x component can be assumed (see Fig. 5).

Hajduk *et al.* (*2*) also investigated the effects of retuning the pulse power to give the maximum excitation or inversion on-resonance. They found that changing the pulse power had bad effects on the frequency profiles. We simulated the same procedure on optimized 90° SLR pulses, adjusting the flip angle (see Table 1). The frequency profiles were not affected

TABLE 2
Signal versus Refocusing Gradient Amplitude with Fixed Flip Angles

T_2 (ms)	Gradient amplitude	Relative refocusing amplitude	Signal gain (%)	Relative refocusing amplitude range
∞	5.0	1.058	+1.38	1.042–1.072
$2L$	5.0	1.028	+0.29	1.012–1.044
L	5.0	0.994	+0.01	0.975–1.011
$L/2$	5.0	0.912	+2.86	0.899–0.924

Note. In the Relative refocusing amplitude range column, the range of relative refocusing amplitudes corresponding to the maximum signal gain $\pm 0.1\%$ is given.

TABLE 3
Signal versus Refocusing Gradient Amplitude with Adjusted Flip Angles

T_2 (ms)	Gradient amplitude	Relative refocusing amplitude	Signal gain (%)	Relative refocusing amplitude range
∞	5.0	1.058	+1.38	1.042–1.072
$2L$	5.0	1.032	+0.42	1.017–1.048
L	5.0	1.008	+0.02	0.990–1.024
$L/2$	5.0	0.924	+1.47	0.912–0.940

Note. In the Relative refocusing amplitude range column, the range of relative refocusing amplitudes corresponding to the maximum signal gain $\pm 0.1\%$ is given.

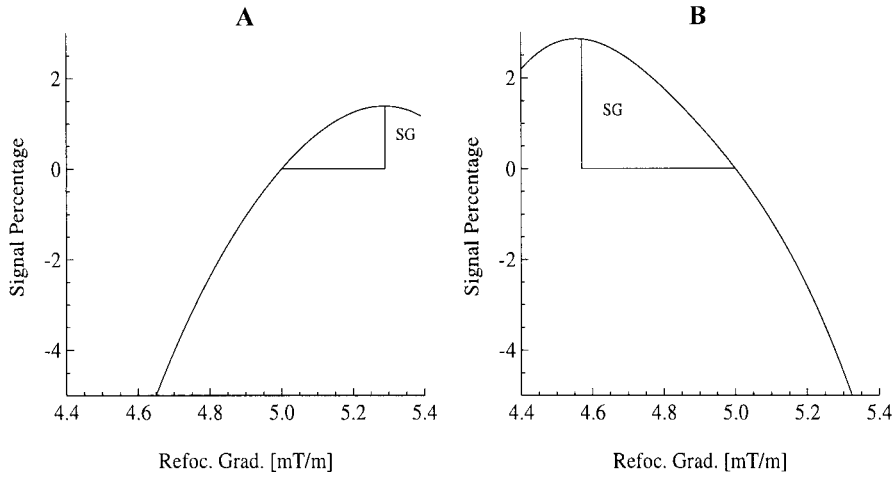

FIG. 6. Signal percentage relative to a pulse with a bandwidth of 2.5 kHz has been calculated for different refocusing gradient amplitudes. It is shown for (A) $T_2 = \infty$; (B) $T_2 = L/2$. SG, signal gain.

by adjusting the pulse power, whereas a remarkable signal gain has been obtained, especially in the case of T_2 time equal to half the length of the pulse (see Fig. 6 and Tables 2–5).

In magnetic resonance, the problem of designing a pulse with a rectangular frequency profile is crucial, as it is very important for many applications to have no distorted profiles. Good results have been already reached by generating pulses without considering relaxation effects. In particular, optimized SLR pulses (*3, 4*) provide a very good solution to this problem. Unfortunately, frequency profiles obtained by performing magnetic resonance of tissues after contrast agent application or magnetic resonance of materials with very short T_2 relaxation times can be very strongly distorted.

Many attempts have been made to adjust the relaxation effects. One of the most widely used methods is to look for the analytical solution of the Bloch equations without neglecting relaxation times. In (*10, 11*), the analytical solution of the Bloch equations has been found in response to a constant-amplitude RF pulse.

The solution has been developed neglecting the longitudinal and/or transverse relaxation times, under specific conditions: exact on-resonance, equal transverse and longitudinal relaxation times, large RF pulse amplitude compared to relaxation rates.

If exact on-resonance and infinite T_1 are the constraints required, it is possible to find a relationship between the magnetization and the RF pulse amplitude in specific regimes of spin behavior (*12*). The pulses generated by using this method are not frequency selective.

Pearlman and Wieczorek (*13*) presented a method to determine RF waveforms for 2D imaging assuming a small variation in time of M_z (small tip angle hypothesis). They operated only on the transverse magnetization, neglecting longitudinal relaxivity, performing a change of variable from time to the *k*-space coordinate. The T_2 relaxivity effect is exponential in time domain only; it is therefore difficult to predict what effect a lack of T_2 correction can have on a given profile.

A different approach for optimizing pulses to include relaxation effects has been performed by Nuzillard and Freeman (*14*). They redesign the RF pulses generated by means of simulating annealing to introduce relaxation effects.

In all of the attempts to consider relaxation effects, the optimization of RF pulses must be performed for specific relaxation times. Usually in clinical MR imaging, the tissues affected by the radiofrequency excitation are characterized by different T_1 and T_2 values. Optimization techniques for a specific relaxation time cannot therefore be used. Nevertheless it is important to be able to estimate the relaxation effects on

TABLE 4
Signal versus Refocusing Gradient Amplitude with Fixed Flip Angles

	2.5 kHz		5.0 kHz		7.5 kHz	
T_2 (ms)	Relative refocusing amplitude	Signal gain (%)	Relative refocusing amplitude	Signal gain (%)	Relative refocusing amplitude	Signal gain (%)
∞	1.058	+1.38	1.041	+2.41	1.029	+2.25
$2L$	1.028	+0.29	1.032	+1.40	1.024	+1.51
L	0.994	+0.01	1.023	+0.67	1.019	+0.90
$L/2$	0.912	+2.86	1.002	+0.002	1.007	+0.14

TABLE 5
Signal versus Refocusing Gradient Amplitude with Adjusted Flip Angles

	2.5 kHz		5.0 kHz		7.5 kHz	
T_2 (ms)	Relative refocusing amplitude	Signal gain (%)	Relative refocusing amplitude	Signal gain (%)	Relative refocusing amplitude	Signal gain (%)
∞	1.058	+1.38	1.041	+2.41	1.029	+2.25
$2L$	1.032	+0.42	1.034	+1.53	1.025	+1.59
L	1.008	+0.02	1.026	+0.85	1.020	+1.01
$L/2$	0.924	+1.47	1.009	+0.08	1.009	+0.24

the magnetization profiles from tissues with relaxation times on the order of the pulse duration.

ACKNOWLEDGMENTS

The authors gratefully acknowledge the financial support of the Deutsche Forschungsgemeinschaf under Grant KL 1093/2-1.

REFERENCES

1. D. G. Norris, H. Lüdemann, and D. Leibfritz, An analysis of the effects of short T_2 values on the hyperbolic-secant pulse. *J. Magn. Reson.* **92,** 94–101 (1991).
2. P. J. Hajduk, D. A. Horita, and L. A. Lerner, Theoretical analysis of relaxation during shaped pulses. I. The effects of short T_1 and T_2. *J. Magn. Reson. A* **103,** 40–52 (1993).
3. J. Pauly, P. Le Roux, D. Nishimura, and A. Macovski, Parameter relations for the Shinnar–Le Roux selective excitation pulse design algorithm. *IEEE Trans. Med. Imaging* **10,** 53–65 (1991).
4. A. Raddi and U. Klose, A generalized estimate of the SLR B polynomial ripples for RF pulse generation. *J. Magn. Reson.* **132,** 260–265 (1998).
5. A. Raddi and U. Klose, Optimized Shinnar–Le Roux RF 180° pulses in fast spin-echo measurements. *J. Magn. Reson. Imaging* **9,** p. 613–620 (1999).
6. G. B. Matson, An integrated program for amplitude-modulated RF pulse generation and re-mapping with shaped gradients. *Magn. Reson. Imaging* **12,** 1205–1225 (1994).
7. K. E. Atkinson, "An Introduction to Numerical Analysis," Wiley, NY (1989).
8. W. H. Press, S. A. Teukolsky, W. T. Vetterling, and B. P. Flannery, "Numerical Recipes in C," Cambridge Univ. Press, Cambridge, UK (1995).
9. J. Machann, F. Schick, O. Lutz, and C. D. Claussen, Optimization of refocusing of selective excitation-pulses. *MAG*MA,* **4**(Suppl.), 277 (1996).
10. H. C. Torrey, Transient nutation in nuclear magnetic resonance. *Phys. Rev.* **76,** 1059–1068 (1949).
11. G. A. Morris and P. B. Chilvers, General analytical solutions of the Bloch equations. *J. Magn. Reson. A* **107,** 236–238 (1994).
12. M. S. Sussman, J. M. Pauly, and G. A. Wright, Design of practical T_2-selective RF excitation (TELEX) pulses. *Magn. Reson. Med.* **40,** 890–899 (1998).
13. J. D. Pearlman and T. J. Wieczorek, Relaxivity corrected response modulated excitation (RME): A T_2-corrected technique achieving specified magnetization patterns from an RF pulse and a time-varying magnetic field. *Magn. Reson. Med.* **32,** 388–395 (1994).
14. J-M. Nuzillard and R. Freeman, Band-selective pulses designed to accommodate relaxation. *J. Magn. Reson. A* **107,** 113–118 (1994).